Hanzlik, R. P., & Tullman, R. H. (1982) *J. Am. Chem. Soc. 104*, 2048–2050.
Husain, M., & Davidson, V. L. (1985) *J. Biol. Chem. 260*, 14626–14629.
Husain, M., & Davidson, V. L. (1987) *J. Bacteriol. 169*, 1712–1717.
Husain, M., Davidson, V. L., Gray, K. A., & Knaff, D. B. (1987) *Biochemistry 26*, 4139–4143.
Janes, S. M., Mu, D., Wemmer, D., Smith, A. J., Kaur, S., Mautry, D., Burlingame, A. L., & Klinman, J. P. (1990) *Science 248*, 981–987.
Kitz, R., & Wilson, I. B. (1962) *J. Biol. Chem. 237*, 3245–3249.
Kumar, M. A., & Davidson, V. L. (1990) *Biochemistry 29*, 5299–5304.
Paech, C., Salach, J. I., & Singer, T. P. (1980) *J. Biol. Chem. 255*, 16302–16305.
Paz, M. A., Gallop, P. M., Torrelio, B. M., & Fluckiger, R. (1988) *Biochem. Biophys. Res. Commun. 154*, 1330–1337.
Salisbury, S. A., Forrest, H. A., Cruse, W. B. T., & Kennard, O. (1979) *Nature 280*, 843–844.
van der Meer, R. A., & Duine, J. A. (1986) *Biochem. J. 239*, 789–791.
van der Meer, R. A., Jongejan, J. A., & Duine, J. A. (1987) *FEBS Lett. 221*, 299–304.
Vellieux, F. M. D., Huitema, F., Groendijk, H., Kalk, K. H., Frank, J. Jzn., Jongejan, J. A., Duine, J. A., Petratos, K., Drenth, J., & Hol, W. G. J. (1989) *EMBO J. 8*, 2171–2178.
Williamson, P. R., Moog, R. S., Dooley, D. M., & Kagan, H. M. (1986) *J. Biol. Chem. 261*, 16302–16305.

Comparison of Reduced and Oxidized Yeast Iso-1-cytochrome *c* Using Proton Paramagnetic Shifts†

Yuan Gao,‡ Jonathan Boyd,§ Gary J. Pielak,*,‖ and Robert J. P. Williams‡

Inorganic Chemistry Laboratory, University of Oxford, Oxford OX1 3QR, U.K., Department of Biochemistry, University of Oxford, Oxford OX1 3QU, U.K., and Department of Chemistry and Program in Molecular Biology and Biotechnology, University of North Carolina at Chapel Hill, Chapel Hill, North Carolina 27599-3290

Received July 11, 1990; Revised Manuscript Received October 5, 1990

ABSTRACT: Dipolar paramagnetic shifts for protons of yeast iso-1-cytochrome *c* have been calculated by using an optimized **g**-tensor and the X-ray crystallographic coordinates of the reduced form of yeast iso-1-cytochrome *c* [Louie, G. V., & Brayer, G. D. (1990) *J. Mol. Biol. 214*, 527–555]. The calculated values are compared with the observed paramagnetic shift determined from over 450 nonequivalent protons that have been assigned in both oxidation states [Gao, Y., Boyd, J., Williams, R. J. P., & Pielak, G. J. (1990) *Biochemistry 29*, 6994–7003]. There is good agreement between the calculated and the experimental data with a few exceptions. This indicates that, overall, the solution structures must be very similar in both the reduced and oxidized states in solution as is the case in crystals. The differences between observed and calculated shift values for the molecule in solution are most readily explained by slight movement of the heme and certain changes in diamagnetic shift due to small rearrangements of a few residues and some considerable changes in a few hydrogen bonds. It is also known that small differences exist between the structures of the two oxidation states in crystals but the hydrogen-bond changes are not so easily observed there. Structural changes from nuclear magnetic resonance data are in reasonable agreement with those deduced from crystallography, but additional information is clearly available concerning changes in hydrogen bonding.

Cytochromes *c* exist in two physiologically important oxidation states. The reduced form is diamagnetic [Fe(II), low spin d^6, $S = 0$], while the oxidized form is paramagnetic [Fe(III), low spin d^5, $S = {}^1/_2$]. Takano and Dickerson (1981a,b) observed specific conformational changes between the X-ray crystal structures of reduced and oxidized tuna cytochrome *c*. These conformational changes are small (<1 Å) and occur in the vicinity of one of the propionic side chains of the heme. The work presented here follows earlier exploratory work based on paramagnetic nuclear magnetic resonance (NMR)[1] shifts for tuna cytochrome *c* (Williams et al., 1985). *Saccharomyces cerevisiae* iso-1-cytochrome *c* is used in the present study because this protein allows easy access to comparative mutational studies. A parallel study of horse heart cytochrome *c* has recently been reported by Feng et al. (1990). We have virtually identical data for horse heart cytochrome *c*, and although our analysis is different, it leads to similar conclusions (unpublished data).

The complete assignment of the C102T variant of yeast iso-1- and horse heart cytochromes *c* in both the oxidized and

† This work was supported by grants from the National Institutes of Health (G.J.P.) and from the Medical Research Council, U.K., and the Royal Society (R.J.P.W.) and by the donors of the Petroleum Research Fund, administered by the American Chemical Society (G.J.P.).

* Corresponding author.
‡ Inorganic Chemistry Laboratory, University of Oxford.
§ Department of Biochemistry, University of Oxford.
‖ University of North Carolina at Chapel Hill.

[1] Abbreviations: EPR, electron paramagnetic resonance; NOE, nuclear Overhauser enhancement; NMR, nuclear magnetic resonance; ppm, parts per million; rms, root mean square.

0006-2960/91/0430-1928$02.50/0

reduced states has been reported (Gao et al., 1990). The C102T variant is studied because it does not exhibit the problems associated with Cys at position 102 (Cutler, 1987). The electron–nuclear interaction resulting from the magnetic moment of the iron-centered unpaired electron in the Fe(III) state alters the chemical shift in the nuclear magnetic resonance spectrum of identical protons between the two oxidation states of the protein in solution. These so-called paramagnetic shifts may be dipolar (pseudocontact) or scalar (Fermi contact) in nature. This difference in the chemical shift of identical protons between the oxidized and reduced forms is defined as the paramagnetic shift. The scalar effect is not discussed here, and therefore, paramagnetic shifts of the heme resonances, most of the amino acid side-chain resonances of the heme ligands (His-18 and Met-80), and the amino acid side-chain resonances of Cys-17 and Cys-14, which form the thioether linkages to the heme, are not analyzed.

The dipolar shift has been given a thorough theoretical interpretation. The magnitude of the shift is given by (Kurland & McGarvey, 1970)

$$\Delta_{pc} = (N\beta^2 S(S+1)/9kTr^3) \times [g_{ax}(3\cos^2\theta - 1) + 1.5g_{eq}\sin^2\theta\cos^2 2\phi] \quad (1)$$

where $g_{ax} = g_z^2 - {}^1/_2(g_x^2 + g_y^2)$, $g_{eq} = g_x^2 - g_y^2$, and the other symbols are as in the papers of Williams et al. (1985) and Feng et al. (1990).

Thus, given a crystal structure—here the coordinates of reduced yeast iso-1-cytochrome *c* as supplied by Dr. G. B. Brayer (Louie & Brayer, 1990) are used—it has been shown that the dipolar shift can be calculated from the **g**-tensor components, starting with electron paramagnetic resonance (EPR) data (Mailer & Taylor, 1972; Williams et al., 1985; Feng et al., 1990). Alternatively, the set of crystal coordinates plus the experimental paramagnetic shift data can be used to search for *g*-values that give the best fit to these data. This will give as output both best-fit calculated shift values and **g**-tensor components characteristic of the iron. These components can then be compared with existing EPR and susceptibility data. In following this procedure it is assumed that there is no change in structure from oxidized to reduced state in solution and that the structure in solution is that of the reduced state in crystals. The observed and calculated values will agree very precisely if this assumption holds. It is known to a high degree of approximation that all four states are very similar both from previous NMR studies (Williams et al., 1985; Feng et al., 1990) and from the crystal structure analyses (Takano & Dickerson, 1981a,b). Differences will then reveal changes between oxidized and reduced forms in the crystal and/or in solution or they will reveal differences between crystal and solution states. Resolution of any resulting complications of interpretation are also discussed.

Experimental Procedures

NMR data for the C102T variant of yeast iso-1-cytochrome *c* were collected at 30 °C as described by Gao et al. (1990). Chemical shifts have an error of ±0.01 ppm. The paramagnetic shift is defined as the chemical shift in the oxidized protein minus that in the reduced protein. These data are summarized in Table I and Figures 1 and 2. The full data set (including data for the heme) is available as supplementary material. Protein coordinates are from the refined (1.23 Å) structure of reduced yeast iso-1-ferrocytochrome *c* (Louie & Brayer, 1990). IUPAC–IUB nomenclature for amino acids (IUPAC–IUB Commission on Biochemical Nomenclature, 1970; IUPAC–IUB Joint Commission on Biochemical Nomenclature, 1985) and the heme group (Commission on the Nomenclature of Biological Chemistry, 1960) is used throughout this article. The use of numeral superscripts to denote substitutent groups of the heme was suggested by Bonnett (1978), and the use of letter superscripts to specify protons on the propionic acid side chains is based on Figure 2 of Chau et al. (1990).

To shorten the computerized search, the **g**-tensor parameters (g_{ax}, g_{eq}, α, β, and γ) from the study of Williams et al. (1985) were used as input along with the derived proton coordinates to calculate the dipolar shifts via eq 1. β represents the tilt of the z axis into the x–y plane, while α and γ describe angles (positive in the clockwise direction) about the old and new orientations of the z axis, respectively. These parameters were then optimized by minimizing X^2, the sum of the squares of

Table I: Side-Chain Protons Used for Calculation of Dipolar Shifts

	1					5					10					15					20
	T	E	F	K	A	G	S	A	K	K	G	A	T	L	F	K	T	R	C	L	Q	C	H	T	V	E	K
β		2	2	1	X	2	1		1	X	1	1	2	2	1	1	1		2	2			1	1	2	1	
γ		X		X	X		X			X	X	1	1	X		1		X	1	1	X	X	1	2			
δ	X	X	1		X	X	X	X			X	X	X	2	2		X		X	2	X	X		X	X	X	
ε	X		1		X	X	X	X			X	X	X	X	2		X		X	X	2	X		X	X		
ζ	X	X	1		X	X	X	X			X	X	X	X	1			X	X	X	X	X	X	X	X		
η	X	X	X	X	X	X	X	X	X	X	X	X	X	X	X	X	X		X	X	X	X	X	X	X	X	

	25					30					35					40					45					
	G	G	P	H	K	V	G	P	N	L	H	G	I	F	G	R	H	S	G	Q	A	E	G	Y	S	Y	T
β	X	X	1	2	2	1	X	2	2	2	2	X	1	2	X	2	1		X	1	1	2	X	2	2	2	1
γ	X	X		X		2	X		X		X	X	3	X	X		X		X	1	X	1	X	X		X	1
δ	X	X		1		X	X		2		1	X	1	1	X	2		X	X	X	X	X	X	2	X	2	X
ε	X	X	X	1		X	X	X	X	X	1	X	X	1	X	1		X	X	2	X		X	2	X		X
ζ	X	X	X	X		X	X	X	X	X	X	X	X	1	X	X	X	X	X	X	X	X	X	X	X	X	X	X
η	X	X	X	X	X	X	X	X	X	X	X	X	X	X	X		X	X	X	X	X	X	X		X		X

	50					55					60					65					70					75
	D	A	N	I	K	K	N	V	L	W	D	E	N	N	M	S	E	Y	L	T	N	P	K	K	Y	I	P
β	2	1	2	1		1	2	1	2	2		2	2	2	2	1	2	2	2	1	2	1	1	1	2	1	1
γ	X	X	X	3			X	2	1	X	X		X	X				X	1	1	X	1			X		
δ		X		1			2	X	2	1		X	2	2		X	X		2	X	2	2			1		1
ε	X	X	X	X			X	X	X	2	X		X	X	1	X			X	X	X	X			1	X	X
ζ	X	X	X	X			X	X	X	2	X	X	X	X	X	X	X		X	X	X	X			X	X	X
η	X	X	X	X	X	X	X	X	X	1	X	X	X	X	X	X	X		X	X	X	X	1	X		X	X

	80					85					90					95					100					
	G	T	K	M	A	F	G	G	L	K	K	E	K	D	R	N	D	L	I	T	Y	L	K	K	A	C	E
β	X	1		1		X	X	2	2	2	2	2	2	1	2	1	2	1	1	2	2	1	2	1	1	2	
γ	X	1		X	X	X	X	1				X		X	X	1	2	1	X	1			X	X			
δ	X	X		X	1	X	X	2		X			2		2	1	X		2			X	X	X	X		
ε	X	X		X	1	X	X	X		X		X		X	X	X	X	X		X			X	X			
ζ	X	X		X	X	1	X	X		X		X	X	X	X	X	X	X		X			X	X	X		
η	X	X	X	X	X	X	X	X	X	X	X	X	X		X	X	X	X		X			X	X	X	X	

[a] The sequence and numbering of iso-1-cytochrome *c* is shown on the top row. Numerals indicate the number of proton-containing moieties utilized (i.e., a methyl group is 1), a blank indicates that the paramagnetic shift for this proton (or protons) is unavailable or that the assignments were not used (side chains of His-18, Met-80, Cys-14, Cys-17, and Thr-102 γ), and X indicates that no such proton is present for the residue. Residue 72 is ε-trimethyllysine.

Table II: g-Tensor Parameters

from EPR	
horse heart cytochrome c^a	
$g_{ax} = 6.05$,	$g_{eq} = -3.50$, $\alpha = \beta = \gamma = 0°$
input values	
from tuna cytochrome c^b	
$g_{ax} = 5.24$,	$g_{eq} = -2.91$, $\alpha + \gamma = 358°$, $\beta = 11°$
optimized values	
C102T variant of yeast iso-1-cytochrome c^c	
$g_{ax} = 4.58$,	$g_{eq} = -2.31$, $\alpha + \gamma = 366°$, $\beta = 9°$
horse heart cytochrome c^d	
$g_{ax} = 4.92$,	$g_{eq} = -1.79$, $\alpha + \gamma = 353°$, $\beta = 14°$

[a] Mailer and Taylor (1972). [b] Williams et al. (1985). [c] This study. [d] Feng et al. (1990).

the differences between the calculated and observed dipolar shifts, while altering systematically the five components of the g-tensor. Three rounds of optimization were performed. In the first round, each angle was incremented by ±5° and each anisotropy was incremented by ±0.05 around the initial values. In the second and third rounds, the increments were ±2°, ±0.02 and ±1°, ±0.01, respectively. The initial and the final optimized values are given in Table II. The optimized g-tensor components differ little from the values determined by others (Mailer & Taylor, 1972; Williams et al., 1985; Feng et al., 1990). Optimization occurred when β was offset by 9° from the original z axis, which is approximately the angle found between the Fe–Met-80 bond and the heme plane. The sum of α and γ is equal to about 360°, indicating that g_x and g_y remain aligned along the diagonal nitrogens of the heme.

At this stage, stereospecific assignments can be inferred for each prochiral entity (e.g., β^1 and β^2 of an Asp) by finding the combination of prochiral chemical shifts in the reduced and oxidized forms that minimizes the difference between the paramagnetic shift and the calculated pseudocontact shift. Many of the stereospecific assignments were then checked by comparison of nuclear Overhauser enhancement (NOE) data from the resonances in question with the stereospecific proton coordinates from the crystal structure. The resulting stereospecific assignments as well as the calculated and observed dipolar shifts are available as supplementary material. These data were used in further rounds of refinement. It is interesting to refer to the different procedure in the analysis of horse heart cytochrome c by Feng et al. (1990), who used a selected set of resonances to fit g-tensor parameters. Judged by the similarity in results, the differences have little effect on the overall impression of the data.

Results

A summary of the calculated dipolar and observed paramagnetic shifts for side-chain protons is given in Table I. (A complete data set is available as supplementary material.) The upper panels of Figures 1 and 2 show the calculated paramagnetic shifts for backbone amide and α protons, respectively. The lower panels of the figures show the difference between calculated and observed values. Paramagnetic shifts are unavailable for amide protons of residues 36, 83, and 84 and for α protons of residues 4, 14, and 83 because these protons remain unassigned in at least one oxidation state. Data for the other classes of protons are of equal or better quality, as can be judged by examination of Table III.

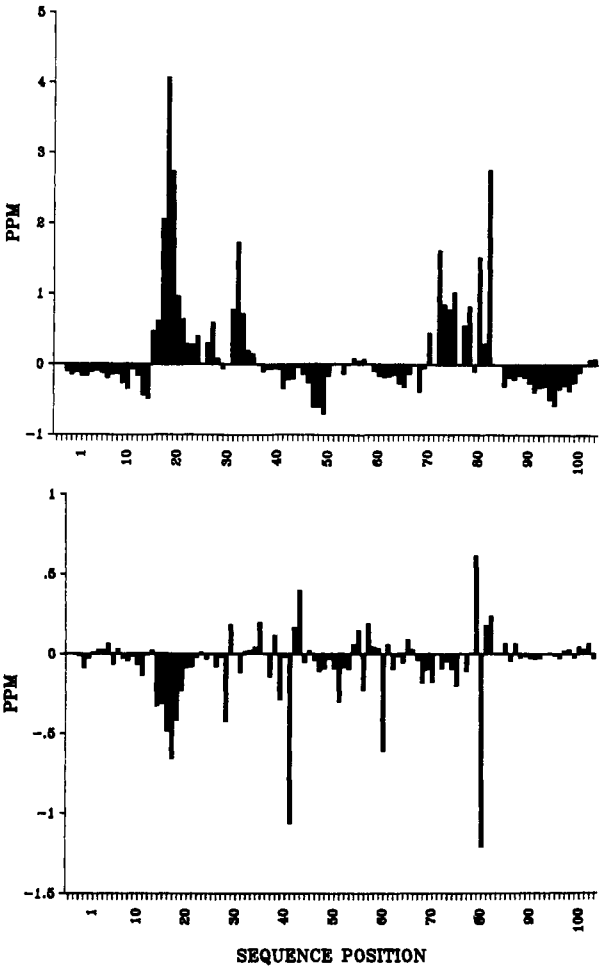

FIGURE 1: Calculated dipolar shift (upper panel) and the difference between the calculated dipolar shift and the observed paramagnetic shift (lower panel) as a function of residue number for backbone amide protons.

Table III: Comparison of Calculated with Observed Values

type of proton	calcd vs obsd			obsd		deviation	
	n	slope	$r^{2\,a}$	avg	rms[b]	avg	rms[c]
amide	99	1.08	0.99	0.21	0.85	−0.05	0.24
α	114	1.05	1.00	0.07	0.89	−0.01	0.21
β	129	0.90	0.99	0.06	0.61	−0.01	0.17
γ	35	0.80	0.96	−0.05	0.86	0.00	0.15
δ^d	47	0.90	0.99	−0.19	0.81	−0.06	0.22
ϵ^d	19	0.88	0.99	−0.29	0.77	0.07	0.22
others	9	1.04	1.00	0.23	0.87	−0.03	0.29
total	452						

[a] Linear correlation coefficient. [b] $[(\sum(\text{calcd shift})^2)/\text{no. of assigned protons}]^{0.5}$. [c] $[(\sum(\text{calcd shift} - \text{obsd shift})^2/\text{no. of assigned protons})^{0.5}$. [d] The calculated shifts for benzoid protons of the fast-flipping residues Phe-3, Phe-36, Phe-82, and Tyr-74 were averaged.

Inspection of Table I and Figures 1 and 2 shows that the experimental dipolar shift data are extensive and that all parts of the protein (both in terms of backbone and side-chain protons) are well represented. Inspection of the upper panels of Figures 1 and 2 indicates that the calculated paramagnetic shifts cover a range of over 7 ppm, from about 5 to −2 ppm. These data are accurate to ±0.02 ppm. Portions of the protein that exhibit large calculated positive or negative pseudocontact shifts are those in the vicinity of the heme. The quality of the fit between calculated and observed values can be gauged by comparing the upper with the lower panels of Figures 1 and 2 and by examining the root mean square differences between them (Table III). Remarkably, it is usually possible to cal-

Table IV: Protons for Which the Difference between Calculated Dipolar Shift and Observed Paramagnetic Shift Is Greater than or Equal to 0.20 ppm

amino acid	difference (ppm)	calcd shift (ppm)	dominant sign of calcd shift	amino acid	difference (ppm)	calcd shift (ppm)	dominant sign of calcd shift
Ser-2			−	Asn-52			±
β^1	0.22	−0.11		α	−0.26	0.21	
β^2	0.22	−0.14		β^2	−0.23	−0.04	
Leu-9			±	Ile-53			±
γ	−0.27	−0.63		α	−0.37	−0.12	
Phe-10			±	Gln-56			±
β	−0.35	−0.33		amide	−0.22	0.04	
δ^1	0.28	0.40		Val-57			±
δ^2	0.53	−0.52		α	−0.34	0.05	
Cys-14			±	β	−0.27	−0.06	
amide	−0.32	−0.48		Trp-59			±
Leu-15			+	ζ^2	−0.23	0.19	
amide	−0.31	0.46		η^2	−0.28	0.49	
α	−0.55	1.47		Asp-60			−
β^1	0.26	0.58		amide	−0.61	−0.16	
β^2	−0.70	0.45		Glu-61			−
δ^2	−0.20	0.35		β^2	−0.25	−0.22	
Gln-16			+	Asn-63			−
amide	−0.48	0.61		β^1	−0.24	−0.11	
α	−0.24	0.51		Met-64			−
β^1	−0.26	0.19		ϵ	0.21	−0.82	
γ	−0.22	0.11		Ser-65			−
Cys-17			+	β^2	−0.31	−0.21	
amide	−0.65	2.06		Glu-66			−
α	−0.72	1.11		β^1	−0.26	0.28	
β^1	0.93	3.38		Leu-68			−
His-18			+	α	−0.33	−0.50	
amide	−0.41	4.07		γ	−0.26	−1.60	
α	−0.44	4.80		δ^2	−0.42	−3.38	
Thr-19			+	Asn-70			+
amide	−0.23	2.73		δ^1	−0.33	0.31	
Lys-27			±	Pro-71			+
β^1	−0.32	1.00		γ^1	0.63	3.13	
β^2	−0.23	0.48		δ^2	0.55	0.99	
Val 28			±	Ile-75			+
amide	−0.42	0.07		β	−0.31	1.17	
Gly-29			±	Thr-78			+
α^1	−0.56	−4.69		β	−0.21	1.30	
α^2	1.50	−1.76		Lys-79			±
Pro-30			±	amide	0.61	−0.09	
α	0.24	0.43		α	−0.33	0.10	
β^2	0.28	−0.67		Met-80			±
Arg-38			−	amide	−1.21	1.52	
δ^2	−0.41	0.06		Ala-81			±
ϵ	0.37	−0.40		β	0.24	0.19	
η	0.37	−0.03		Phe-82			±
His-39			−	amide	0.24	2.77	
amide	−0.29	0.06		α	0.54	−0.02	
α	0.35	−0.06		δ^{1+2}	1.21	−0.55	
Ser-40			−	Leu-85			±
α	0.29	−0.17		δ^1	0.227	−0.80	
Gly-41			−	Leu-94			−
amide	−1.06	−0.34		δ^2	0.29	−1.89	
Ala-43			−	Leu-98			−
amide	0.40	−0.20		β^1	0.29	−0.52	
Tyr-46			−	β^2	−0.51	−0.36	
δ^2	−0.41	−1.05		δ^1	−0.54	−1.31	
ϵ^1	0.55	−1.25		δ^2	−0.53	−2.33	
Ala-51			−				
amide	−0.30	−0.01					

culate dipolar shifts of ±0.10 ppm to within ±0.02 ppm at distances up to 20 Å from the iron. Regions in which the calculated and observed differences match most directly are known to be the most rigid parts of the molecule (i.e., residues 1–9, 18–26, 44–50, and 88–102). Although the agreement between experimental and calculated values is very good, there are places along the backbone where differences are very much greater than the experimental error in the paramagnetic shift (±0.02 ppm). In places the differences can exceed 1 ppm. The root mean square deviation between calculated and observed values for all types of protons is about 0.2 ppm. Protons whose calculated and observed values differ by more than this amount are listed in Table IV and discussed below.

Discussion

Why Might There Be Differences between Calculated and Observed Shifts? (1) There could be an error in resonance assignments. It is unlikely that the assignments are in error since both the C102T protein and horse cytochrome *c* in both oxidation states have been assigned in this laboratory (Gao et al., 1990). The protein from horse was also assigned by Feng et al. (1989) and Wand et al. (1989), who have also

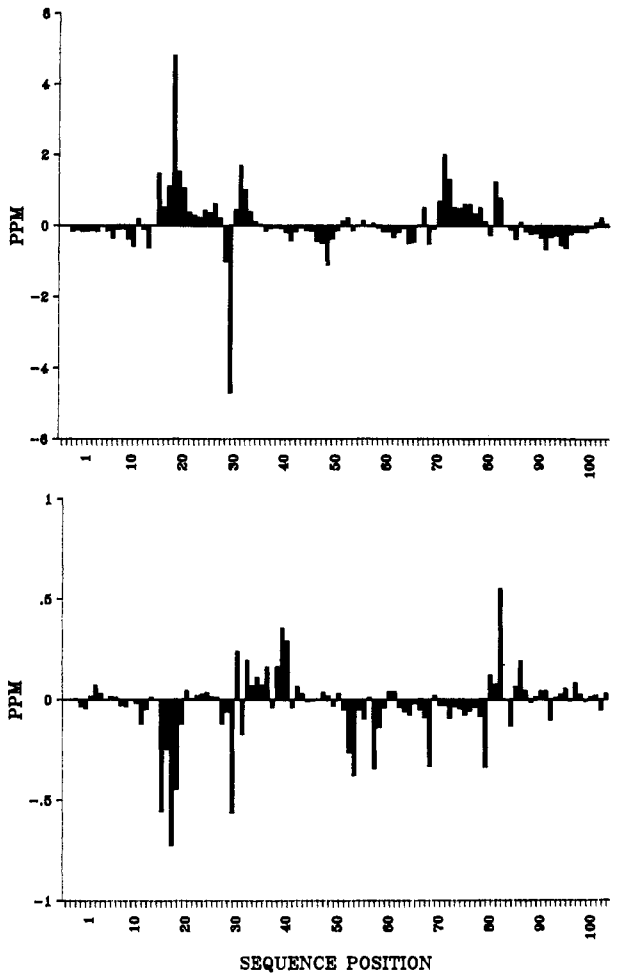

FIGURE 2: Calculated dipolar shifts (upper panel) and the difference between the calculated dipolar shift and the observed paramagnetic shift (lower panel) as a function of residue number for α protons. Data are presented for only one glycine proton. Calculated and calculated minus observed values for the other glycine protons (in ppm) are as follows: Gly-1, −0.18, 0.01; Gly-6, −0.30, 0.02; Gly-23, 0.18, 0.03; Gly-24, 0.52, 0.03; Gly-29, −3.26, 1.50; Gly-34, 0.0, 0.11; Gly-41, −0.29, 0.04; Gly-45, −0.11, 0.02; Gly-77, 0.35, −0.06; Gly 84, 0.20, −0.01.

analyzed paramagnetic shift data for horse cytochrome *c* (Feng et al., 1990). Agreement is excellent in all respects. (We are very grateful for an exchange of data, which established confidence).

(2) The C102T mutation could introduce a minor structural change, thereby invalidating detailed comparison of paramagnetic shift data for this variant with the X-ray crystal structure coordinates for the wild-type protein. However, analysis of paramagnetic shift (Pielak et al., 1988) and NOE data (Gao et al., 1990) indicates that the structures of the C102T variant and the wild-type protein are extremely similar.

(3) There could be motional averaging if prochiral protons (e.g., $\delta 1$ and $\delta 2$ of a Tyr or Phe) are in fast exchange, rendering the chemical shifts of these protons identical (Campbell et al., 1975; Wüthrich & Wagner, 1975). For this case there will be a discrepancy between calculated and observed data because each proton will possess a unique calculated pseudocontact shift. Examples are Phe-36, Tyr-74, and Phe-82. For these three aromatic side chains the average experimental shift for the two prochiral protons is close to the mean of the two as calculated. Similar arguments could apply to Gly (2 α's), Leu (2 methyl groups), Val (2 methyl groups), and many β and γ protons if there is free rotation. In fact, motional averaging is not observed for any prochiral methyl group since each of the shifts is unique. However, there is obviously averaging for many exposed methylene side chains. Note that the potentially exchangeable side-chain resonances of surface Lys, Arg, Asp, and Glu residues are not frequently observed in two-dimensional NMR data. Presumably chemical exchange with solvent broadens these resonances, precluding their detection. Many, but not all, side-chain amide protons are observed.

(4) There could be differences between oxidation states and/or differences between solution and crystal structures. These possibilities are discussed in the next sections.

For Large Portions of the Protein There Is Very Good Agreement between Calculated and Observed Shifts. Data concerning quantitative evaluation of calculated and observed shifts are given in Table III. When calculated (x) and observed (y) shifts are plotted, the slope and the linear correlation coefficient are close to one for all the type of protons examined, indicative of a close correlation between calculated and observed values. The close agreement between calculated and observed shifts indicates that there can be little difference between crystal and solution structures or between the two oxidation states. This conclusion is in accord with the qualitative analysis of proton NOE data (Gao et al., 1990), with NMR studies of both tuna (Williams et al., 1985; Gao et al., 1989) and horse (Feng et al., 1989; Wand et al., 1989) cytochromes *c*, and with the crystallographic data of Takano and Dickerson (1981a,b).

There Is a Small Change in the Position of the Heme. There are several places in the primary sequence where the calculated pseudocontact shift changes sign (Figures 1 and 2). These represent regions where the backbone crosses a part of space where the dipolar shift is equal to zero in eq 1. The calculated dipolar shift for amide protons changes sign nine times and there are ten sign changes for α protons—overwhelmingly at closely related positions in the sequence. Of the over 450 calculated paramagnetic shifts, there are 35 sign discrepancies between calculated and observed data. Twenty-two of these discrepancies occur within one residue of a change in sign of the calculated dipolar shift for amide or α protons. These observations suggest that the heme has shifted slightly either between solution and crystal or between oxidized and reduced states. The latter explanation is more probable because protons from residues near the heme periphery (14–19, 28, 38, 41, 79–82; Table IV) also exhibit discrepancies between calculated pseudocontact shift and observed paramagnetic shift. The observation of several amide resonances among this group of protons is also consistent with a small movement of the heme that alters the hydrogen-bonding network at the heme periphery. Alterations at the heme periphery were also observed crystallographically (Takano & Dickerson, 1981a,b). Because discrepancies near sign changes are at least partly caused by movement of the heme, it is difficult to separate exactly changes in protein structure from movement of the heme.

Next, large discrepancies ($>\pm 0.2$ ppm) between experimental and calculated shifts (Table IV) are analyzed. Discrepancies occurring in portions of the protein near a change in sign of the calculated shift are ignored because in these regions the shift is very sensitive to small errors in the coordinates. Residues 9, 10, 14, 27–30, 53, 56, 57, 59, 79–82 and 85 fall into this category (rightmost column of Table IV).

Of the protons listed in Table IV, some have very large calculated shifts so that a shift difference of ± 0.2 ppm may be difficult to interpret. A large shift indicates that the residue is close to the heme, and as discussed above, relative to the

heme there appears to be a small change in coordinates. In particular, residues 15–19, 46, 75, 94, and 98 are excluded from discussion. Interest then centers on residues 2, 38–43, 51, 52, and 60–71. The observation on Ser-2 has been confirmed in several variants of yeast iso-1-cytochrome *c* (data not shown) and implies that the Ser side chain rotates or alters its hydrogen bonding from crystal to solution. Ser-2 is in the N-terminal helix and so far from the heme that a redox-state-dependent change is unlikely.

Discrepancies between Calculated Pseudocontact Shifts and Observed Paramagnetic Shifts for Protons from Residues 38–43, 51, 52, 60, 61, 63–66, 68, 70, and 71 Are Indicative of Changes in Hydrogen Bonding between Oxidation States. The chemical shift of backbone protons is very sensitive to diamagnetic shifts brought about by changes in hydrogen bonding in the absence of movement of aromatic residues (Gao et al., 1990; Wagner et al., 1983). Therefore, large differences between calculated and observed values for amide protons where much smaller changes in α-proton discrepancies are found probably reflect changes in hydrogen bonding. The predominance of such amide protons in the region 38–43 indicates that changes in hydrogen bonding occur in this region. From examination of the crystal structure (Takano & Dickerson, 1981a,b; Louie et al., 1988; Louie & Brayer, 1990), residues 38–43 and 52 are involved in the interaction of the protein with the propionic side chain emanating from heme carbon 17 of the heme. For *S. cerevisiae* iso-1-ferrocytochrome *c* (Louie & Brayer, 1990), the ϵ proton of Arg-38, the carbonyl oxygen of His-39, and the main-chain amide of Gln-42 form hydrogen bonds to a buried water molecule, which is in turn hydrogen-bonded to heme propionate oxygen 17^{3a}. Heme propionate oxygen 17^{3a} also forms hydrogen bonds with the hydroxyl proton of Tyr-48 and a second buried water molecule. The amide of Gly-41, the side-chain amide of Asn-52, and the position 1 proton of Trp-59 form hydrogen bonds to the other oxygen of this propionate (17^{3b}). The other exchangeable side-chain proton of Asn-52 along with the hydroxyl protons of Tyr-67 and Thr-78 form hydrogen bonds to a third buried water molecule. The amide proton of Gly-41 exhibits the largest difference between calculated and observed values of any main-chain amide proton. In the model for the redox-linked conformational change in tuna cytochrome *c* (Takano & Dickerson, 1981b), the distance between the amide of Gly-41 and the side chain of Asn-52 shortens from 3.5 to 3.0 Å on going from the oxidized to reduced form. The simplest explanation for shift discrepancies occurring between residues 38 and 43 is that the hydrogen-bond network has been rearranged in this region. The series of discrepancies between residues 60 and 71 is now readily interpreted. These residues form a distorted α-helix and occur in a region with low evolutionary conservation (Cutler et al., 1987). This region also exhibits large changes in chemical shift between species (Gao et al., 1990). Discrepancies between calculated and observed dipolar shifts in this region, again stressing changes of peptide amides, indicate an alteration for the helix. Undoubtedly this change is partly due to the above hydrogen-bond network through the aromatic side chains of Trp-59, Tyr-67, and Tyr-74, especially their side-chain exchangeable protons.

Confirmation of the changes discussed above was sought. NOE data show that the relationship between the amide of Gly-41 and residues such as Asn-52 and Tyr-48, for example, changes somewhat between the two oxidation states (data not shown). However, analysis of paramagnetic shifts is much more sensitive in detecting alterations in hydrogen-bond networks.

Comparison with Other Studies. The original study on the comparison of calculated pseudocontact shift to observed paramagnetic shifts for tuna cytochrome *c* is that of Williams et al. (1985). In this study, structural changes occurring between crystals and solution were stressed. Although not nearly as many assignments were available, the authors concluded that there were some small redox-state-dependent changes near the heme propionate emanating from heme carbon 17, at the heme edge near heme methyl 3^2, and in the C-terminal helix. The effect in the C-terminus may be unique because of Trp-33, which is unique to this protein. Therefore, the conclusions of the present study are in accord with the earlier study by Williams et al. (1985) although it now appears that changes in structure between the different oxidation states in solution are more important than changes between the crystalline and solution states. The other detailed study is that of Feng et al. (1990), who exploited a subset of α-proton assignments to calculate best-fit **g**-tensor parameters for horse cytochrome *c* and then used the parameters to calculate the pseudocontact shift. In the present study, all proton assignments (except for those that experience significant contact shift) were used to calculate **g**-tensor parameters. The former basis set might be expected to overestimate discrepancies, especially those involving exchangeable protons, while the latter might be expected to underestimate them. However, both the study of Feng et al. (1990) and the present study come to essentially the same conclusions.

Conclusions

There is not a major conformational change upon changing the oxidation state of cytochrome *c* in solution. However, there are changes in several parts of the NMR spectrum of the protein that could be due to either changes from crystal to solution structure or redox-linked conformational changes. It is very possible that there is a small change in the position of the heme on redox reactions both in crystals and in solution. There is clearly a large redox-linked change detected around Gly-41 and residues 51 and 52 and linked changes around the sequence 60–71. There are many smaller changes that are probably significant. The similarity between our results on yeast iso-1-cytochrome *c* and those for the horse heart protein (Feng et al., 1990; Y. Gao, J. Boyd, G. J. Pielak, and R. J. P. Williams, unpublished observations) and the tuna protein (Williams et al., 1985) show that the redox-state changes observed are a general feature of eukaryotic cytochromes *c*. Coupling of the redox-state changes with changes in hydrogen-bonding networks is of particular significance and will be examined in a further paper on a number of variant yeast iso-1-cytochromes *c*.

Acknowledgments

We thank Colin Greenwood and Adrian Thompson for access to and assistance in the use of their fermentation facilities. R.J.P.W. is a member of the Oxford Interdisciplinary Center for Molecular Studies.

Supplementary Material Available

Two tables giving the calculated dipolar shifts for yeast iso-1-cytochrome *c* and stereospecific assignments for the reduced and oxidized protein, including the heme (27 pages). Ordering information is given on any current masthead page.

Registry No. Cytochrome *c*, 9007-43-6.

References

Campbell, I. D., Dobson, C. M., & Williams, R. J. P. (1975) *Proc. R. Soc. London, Ser. B 189*, 503–509.

Chau, M.-H., Cai, M. L., & Timkovich, R. (1990) *Biochemistry 29*, 5076-5087.
Commision on the Nomenclature of Biological Chemistry (1960) *J. Am. Chem. Soc. 82*, 5545-5584 (see page 5582).
Cutler, R. L., Pielak, G. J., Mauk, A. G., & Smith, M. (1987) *Protein Eng. 1*, 95-99.
Feng, Y., Roder, H., Englander, S. W., Wand, A. J., & Di Stefano, D. L. (1989) *Biochemistry 28*, 195-203.
Feng, Y., Roder, H., & Englander, S. W. (1990) *Biochemistry 29*, 3494-3504.
Gao, Y., Lee, A. D. J., Williams, R. J. P., & Williams, G. (1989) *Eur. J. Biochem. 182*, 57-65.
Gao, Y., Boyd, J., Williams, R. J. P., & Pielak, G. J. (1990) *Biochemistry 29*, 6994-7003.
IUPAC-IUB Commission on Biochemical Nomenclature (1970) *J. Biol. Chem. 245*, 6489-6497.
IUPAC-IUB Joint Commission on Biochemical Nomenclature (1985) *J. Biol. Chem. 260*, 14-41.
Kurland, R. J., & McGarvey, B. R. (1970) *J. Magn. Reson. 2*, 286-301.
Louie, G. V., & Brayer, G. D. (1990) *J. Mol. Biol. 214*, 527-555.
Louie, G. V., Hutcheon, W. L., & Brayer, G. D. (1988) *J. Mol. Biol. 199*, 295-314.
Mailer, C., & Taylor, C. P. S. (1972) *Can. J. Biochem. 85*, 1048-1055.
Pielak, G. J., Boyd, J., Moore, G. R., & Williams, R. J. P. (1988) *Eur. J. Biochem. 177*, 167-177.
Takano, T., & Dickerson, R. E. (1981a) *J. Mol. Biol. 153*, 79-94.
Takano, T., & Dickerson, R. E. (1981b) *J. Mol. Biol. 153*, 95-115.
Wagner, G., Pardi, A., & Wüthrich, K. (1983) *J. Am. Chem. Soc. 105*, 5948-5949.
Wand, A. J., Di Stefano, D. L., Feng, Y., Roder, H., & Englander, S. W. (1989) *Biochemistry 28*, 186-194.
Williams, G., Clayden, N. J., Moore, G. R., & Williams, R. J. P. (1985) *J. Mol. Biol. 183*, 447-460.
Wüthrich, K., & Wagner, G. (1975) *FEBS Lett. 50*, 265-268.

Purification and Characterization of Dihydroorotate Dehydrogenase from the Rodent Malaria Parasite *Plasmodium berghei*†

Jerapan Krungkrai,‡ Anthony Cerami,* and Graeme B. Henderson§
Laboratory of Medical Biochemistry, The Rockefeller University, 1230 York Avenue, New York, New York 10021
Received April 25, 1990; Revised Manuscript Received November 26, 1990

ABSTRACT: Dihydroorotate dehydrogenase (DHODase) has been purified 400-fold from the rodent malaria parasite *Plasmodium berghei* to apparent homogeneity by Triton X-100 solubilization followed by anion-exchange, Cibacron Blue F3GA-agarose affinity, and gel filtration chromatography. The purified enzyme has a molecular mass of 52 ± 2 kDa on sodium dodecyl sulfate-polyacrylamide gel electrophoresis and of 55 ± 6 kDa by gel filtration chromatography, and it has a pI of 8.2. It is active in monomeric form, contains 2.022 mol of iron and 1.602 acid-labile sulfurs per mole of enzyme, and does not contain a flavin cofactor. The purified DHODase exhibits optimal activity at pH 8.0 in the presence of the ubiquinone coenzyme CoQ_6, CoQ_7, CoQ_9, or CoQ_{10}. The K_m values for L-DHO and CoQ_6 are 7.9 ± 2.5 μM and 21.6 ± 5.5 μM, respectively. The k_{cat} values for both substrates are 11.44 min^{-1} and 11.70 min^{-1}, respectively. The reaction product orotate and an orotate analogue, 5-fluoroorotate, are competitive inhibitors of the enzyme-catalyzed reaction with K_i values of 30.5 μM and 34.9 μM, respectively. The requirement of the long-chain ubiquinones for activity supports the hypothesis of the linkage of pyrimidine biosynthesis to the electron transport system and oxygen utilization in malaria by DHODase via ubiquinones [Gutteridge, W. E., Dave, D., & Richards, W. H. G. (1979) *Biochim. Biophys. Acta 582*, 390-401].

Dihydroorotate dehydrogenase (DHODase,[1] L-5,6-dihydroorotate:oxygen oxidoreductase, EC 1.3.3.1), the fourth sequential enzyme in the de novo biosynthesis of pyrimidines, catalyzes the oxidation of dihydroorotate (DHO) to orotate (OA). In many bacterial systems, the DHODase is membrane bound, and its action is intimately linked to the cell's respiratory systems (Karibian & Couchoud, 1974; Larsen & Jensen, 1985). Similarly, in a variety of eukaryotic cells, the enzyme is physically associated with the membrane of the mitochondrion, and again, its action appears to be linked to respiratory electron transport (Jones, 1980; Chen & Jones, 1976; Forman & Kennedy, 1978; Hines et al., 1986; Gero & O'Sullivan, 1985). In contrast, a cytosolic form of DHODase has been isolated from the trypanosomatid protozoans *Crithidia fasciculata* and *Trypanosoma brucei* (Pascal et al., 1983; Pascal & Walsh, 1984), and a similar enzyme has been found in *Escherichia coli* (Larsen & Jensen, 1985).

The parasitic protozoa responsible for human malaria are totally dependent on de novo biosynthesis for their pyrimidine

† This work was supported by a grant from the Rockefeller Foundation, RF 88062. J.K. is a King of Thailand Biomedical Fellow.
* To whom correspondence should be addressed.
‡ Current address: Department of Biochemistry, Faculty of Medicine, Chulalongkorn University, Bangkok 10330, Thailand.
§ Dr. Graeme B. Henderson died in an accident while this paper was in preparation.

[1] Abbreviations: DHODase, dihydroorotate dehydrogenase; L-DHO, dihydroorotate; L-OA, orotate; 5-F-OA, 5-fluoroorotate; DCIP, dichlorophenolindophenol; FPLC, fast protein liquid chromatography.

0006-2960/91/0430-1934$02.50/0